ANALYSIS OF SIMULATED DIFFUSION AND ADSORPTION WITH AN ANALYTICAL MODEL FOR FLUORESCENCE CORRELATION SPECTROSCOPY

Hong Bok Lee

Department of Chemistry, University of Iowa, USA

Email: hongbok-lee@uiowa.edu

Abstract

Fluorescence correlation spectroscopy (FCS) is a powerful tool to predict molecular diffusivity in femtoliter observation volume. The applicable analytical model in 3-D for porous chromatographic environment has been introduced to evaluate in this contribution. Regarding chromatographic environment, it is important to understand and characterize both diffusion and adsorption-desorption kinetics at interfacial area between mobile and stationary phases. In this contribution, a demonstration of a newly designed analytical model for FCS was presented that can predict simulated diffusion and adsorption-desorption kinetics in 3-D matrix. This work was motivated by a previous 2-D analytical solution study. The range of desorption rate (800–1000 1/s) was found to be where the analytical model can predict the molecular dynamics most accurately and precisely.

Key Words - confocal microscopy, computer simulation, Monte Carlo simulation, FCS

1. Introduction

The theoretical modeling for diffusion and adsorption kinetics using of fluorescence correlation spectroscopy (FCS) was developed earlier in 1970's by Elson and Magde[1-3]. The further modifications of theoretical model FCS and various applications of using FCS have been conducted for observing various cases of diffusion and kinetics depending on the unique investigation purposes[4-11]. Investigation of interfacial area between mobile phase and stationary phase has been required while most chemical separation studies were conducted based on analyzing column efficiency from bulk separation experiments[12]. One of the most challenging but required tasks is to understand the molecular dynamics in chromatographic interfacial areas. Single-molecule spectroscopy in the past studies has vigorously revealed the problematic issues such as band broadening and peak tailing[13]. The discovery of heterogeneous strong adsorption was the main concern of the peak tailing because of the organic modified layer, for example, C_{18} (chloro(dimethyl)octadecylsilane)) on silica surface. The pore surface was always exposed by both silanol groups (SiOH) and dissociated silanols (SiO^-)[13, 14]. However, surface diffusion and sorption kinetics on pore surface simultaneously play the central role of the mass transportation in the real chemical separation[15, 16]. Therefore, it is important to develop a theoretical model or an analytical model to interpret the diffusion and adsorption-desorption kinetics before planning to observe the molecular dynamics. Single-molecule spectroscopy allows us to characterize single-molecule dynamics with picomolar concentration of fluorophore solution, but there could be a limitation of collecting molecular dynamic information for a short amount of time. Rather than measuring the adsorption time and desorption time manually based on the single-molecule level acquisition, using fluorescence correlation spectroscopy (FCS) with a higher sample concentration and a proper theoretical model should be thought as the more efficient way to collect a larger amount of molecular dynamics information; the sample for FCS is usually nanomolar concentration that allows to acquire a sufficient number of fluorophore dynamics in a relatively short amount of time (several seconds–minutes). FCS has been widely used because of its capability to predict molecular diffusivity in a femtoliter observation volume[5-7, 17-20]. In order to test a newly designed analytical model[21], it is necessary to review the theoretical background of the previous theoretical autocorrelation functions and need to construct Monte Carlo simulation to generate theoretical diffusion and adsorption-desorption kinetics.

The simulation in this contribution generated virtual fluorescence fluctuation data by combining diffusion and adsorption events. Based on the fluctuation data, autocorrelation curves were constructed, and they were evaluated by nonlinear curve fitting (nonlinear least squared fit). The computation method was motivated by the diffusion and adsorption simulation work in 2-D confocal environment[22]. The simulated observational volume and the intensity distribution were based on Gaussian distribution. The simulation was implemented by developing

home-written MATLAB codes, generating Monte Carlo simulation. The newly designed analytical model was tested to see if it can be applied for observing diffusion and adsorption-desorption kinetics and was evaluated by statistical analysis.

2. Theoretical background of modeling the autocorrelation function

In short, Elson and Magde in 1974 has shown that the chemical reaction was based on between DNA (A) and EtBr (B) to form the complex (C) with rate constants k_1 and k_{-1} as shown the chemical equilibrium as below[1-3].

$$A + B \underset{k_{-1}}{\overset{k_1}{\rightleftarrows}} C$$

, and the general solution can be described with the Fourier transformation with the variable, $\boldsymbol{v} = (v_x, v_y, n)$ where $n = 0,1,2,..$

$$\frac{\partial C_l(\boldsymbol{v},\tau)}{\partial \tau} = \sum_{k=1}^{m} M_{lk} C_k(\boldsymbol{v},\tau)$$

where

$$\boldsymbol{M} = \begin{vmatrix} -(v^2 D_A + k_1 C_B) & -k_1 C_A & k_{-1} \\ -k_1 C_B & -(v^2 D_B + k_1 C_A) & k_{-1} \\ k_1 C_A & k_1 C_A & -(v^2 D_C + k_{-1}) \end{vmatrix}.$$

However, Wirth *et al.* (2001) pointed out that the specific case of binding introduced in the paper of Elson and Magde (1974) was not applicable for studying rare strong adsorptions at chemical interfaces[22]. Wirth *et al.* (2001) have modified and provided the different assumptions and matrix elements for appropriate conditions of the rare strong adsorptions[22]. Based on the chemical equilibrium and the conditions what Wirth *et al.* (2001) provided, *A* is adsorption site (in C18 layers) which is nonfluorescent and no diffusion ($\epsilon_A = 0$ and $D_A = 0$, respectively), *B* is the diffusing fluorophore ($D_B = D$), and *C* is the adsorbed fluorophore with no diffusion ($D_C = 0$). The concentration of diffusing fluorophores, $\langle C_B \rangle$, is very low so the adsorption sites are not saturated. The other key assumptions were made for $D_B / \left(\frac{\omega_0}{2}\right)^2 \gg k_1 \langle C_A \rangle$ and $k_{-1} \gg k_1 \langle C_A \rangle$ meaning that the strong adsorption is not significantly frequently occurred in a step of time and the rate of desorption (k_{-1}) is significantly greater than the rate of adsorption ($k_1 \langle C_A \rangle$), respectively. The matrix, $\boldsymbol{M}$, is expressed by Wirth *et al.* (2001) as following matrix[22].

$$\boldsymbol{M} = \begin{vmatrix} -k_1 C_B & -k_1 C_A & k_{-1} \\ k_1 C_B & -(v^2 \boldsymbol{D} + k_1 C_A) & k_{-1} \\ k_1 C_A & k_1 C_A & -k_{-1} \end{vmatrix}$$

Based on those terms, Wirth *et al.* (2001) derived $G(\tau)$ in 2-D system as below.

$$G(\tau) = \epsilon_B Q_B \langle C_B \rangle G_{BB}(\tau) + \epsilon_C Q_C \langle C_C \rangle G_{CC}(\tau)$$

where $G_{BB}(\tau) = \frac{1}{1+\frac{\tau}{\tau_D}}$ and $G_{CC}(\tau) = exp(-k_{-1}\tau)$.

Because the spherical C_{18} silica particle is 3-D environment, the $G_{BB}(\tau)$ is needed to be modified into 3-D rather than 2-D. The paper of Aragon and Pecora (1976) provided the theoretical model of 3-D Gaussian profile[23], so $G_{BB}(\tau)$ can be expressed as the pure diffusion model as below equation[17, 24].

$$G_{BB}(\tau) = \left(1 + \frac{\tau}{\tau_D}\right)^{-1} \left(1 + \frac{\tau}{S^2 \cdot \tau_D}\right)^{-1/2}$$

where diffusion coefficient, D, can be introduced to the following equation with characteristic diffusion time, $\tau_D = \frac{{\omega_0}^2}{4D}$. τ means correlation time. The autocorrelation function for diffusion model in 3-D without adsorption terms can be expressed to the following equation, and this will be called simply "pure diffusion model".

$$G(\tau) = \frac{1}{N}\left(1 + \frac{4D\tau}{{\omega_0}^2}\right)^{-1} \left(1 + \frac{4D\tau}{{z_0}^2}\right)^{-1/2}$$

where ω_0 is lateral beam radius, z_0 is axial beam radius.

After normalization for the value of $G(\tau)$ with fractional terms $f_B = \frac{\langle C_B \rangle}{\langle C_B \rangle + \langle C_C \rangle}$ and $f_C = \frac{\langle C_C \rangle}{\langle C_B \rangle + \langle C_C \rangle}$, the general solution can be expressed as below.

$$G(\tau) = \epsilon_B Q_B f_B \left(1 + \frac{\tau}{\tau_D}\right)^{-1} \left(1 + \frac{\tau}{S^2 \cdot \tau_D}\right)^{-1/2} + \epsilon_C Q_C f_C exp(-k_{-1}\tau)$$

where $S = \frac{z_0}{\omega_0}$.

Finally, the autocorrelation function for data analysis can be expressed as following equation[21] which will be simply called "adsorption model", assuming that the spectroscopic properties have $\epsilon_B Q_B = \epsilon_C Q_C = 1/N$, where N represents the average emission photons in the observational volume.

$$G(\tau) = \frac{f_B}{N}\left(1 + \frac{4D\tau}{{w_0}^2}\right)^{-1} \cdot \left(1 + \frac{4D\tau}{{z_0}^2}\right)^{-1/2} + \frac{f_C}{N} exp(-k_{-1}\tau)$$

where $f_C = 1 - f_B$. Once the simulation of virtual fluorescence fluctuation data under the realistic experimental condition of FCS was generated, the autocorrelation curve was constructed using the fluctuation data. The experimental autocorrelation curve can be expressed as following equation[5, 25].

$$G(\tau) = \frac{\langle \delta F(t) \delta F(t+\tau) \rangle}{\langle F(t) \rangle^2}$$

where $\delta F(t) = F(t) - \langle F(t) \rangle$ and $\langle\ \rangle$ denotes the average over time, t. $\langle F(t) \rangle$ represents mean fluorescence intensity over t. The autocorrelation decay behavior includes information of molecular dynamics through the observation volume in FCS. The theoretical model fits the

autocorrelation curve to extract the parameters of interest such as diffusion time (τ_D) or diffusion coefficient (D), and desorption rate (k_{-1}). The comparison between simulation input parameter and output parameter from the nonlinear curve fits was evaluated to see how accurate and precise desorption rate estimations.

3. Combination of diffusion and sorption kinetics into computer simulation

The computer simulation of diffusion was constructed based on generating molecular random walks such as "hopping" on 3-D Cartesian coordinates. Based on the information of molecular locations over the time, the virtual fluorescence fluctuation was determined following the Gaussian intensity distribution inside the observational volume. The diffusion simulation was implemented by writing MATLAB codes and the nonlinear curve fit analysis with the theoretical autocorrelation functions was conducted using the software, OriginPro. For simulating the confocal system in a realistic experimental condition, the input values of beam size were 0.2 μm and 1.0 μm for lateral and axial beam radius respectively. For simulating a realistic data collection, a single data trace of virtual fluorescence intensity consisted of 65535 data points. To illustrate molecular dynamics, the randomly located initial data points were positioned to the next steps within a 3-D Gaussian distribution.

$$variance = 2n \cdot D \cdot dwell$$

where $variance$ means the variance of each step length ($L(t)$), $dwell$ means dwell time or bin of each step, and n is the dimension of the environment[22]. The dwell time in the simulation was 2 μs. The whole system here was limited to a spherical wall, and it was four times larger than the axial beam radius. The wall radius was set to 4 μm, R_{wall}. At the initial placement ($t_0 = 0$), each molecule position was randomly generated inside the spherical wall as following the spherical coordinate system[22].

$$x(t_0) = rand \cdot sin(\varphi) \cdot cos(\theta)$$
$$y(t_0) = rand \cdot sin(\varphi) \cdot sin(\theta)$$
$$z(t_0) = rand \cdot cos(\varphi)$$

where random numbers for $rand$, θ, and φ are generated with uniform distribution in the range of $0 \le rand \le 0.99R_{wall}$, $0 \le \theta \le 2\pi$, and $-\frac{\pi}{2} \le \varphi \le \frac{\pi}{2}$ respectively.

All simulation experiments here generated 600 diffusing molecules in a spherical shell with 4 μm radius which makes a realistic 3.7 nM concentration of the solution. Considering those conditions, another random number set was generated following a normal distribution for adding the displacement of next steps. For the fundamental explanation of molecular diffusive motion, Fick's second law should be referred which is described as following equation.

$$\frac{\partial p}{\partial t} = D\frac{\partial^2 p}{\partial x^2}$$

where $p(x,t)$ is the probability distribution of the particle's location (x) at the time (t). Assuming the condition in 1-D of $p(x,t_{k-1}) = \delta(x - x_{k-1})$ and $\lim_{x\to\pm\infty} p(x,t) = 0$, the normal distribution can be described as the following solution.

$$p(x,t) = \frac{\exp\left(-\frac{(x-x_{k-1})^2}{4(t-t_{k-1})D}\right)}{\sqrt{4\pi(t-t_{k-1})D}}$$

where the mean is x_{k-1} and the variance is $2(t - t_{k-1})D$. The position in x, y and z of a molecule after k steps of 3-D diffusion, (x_k, y_k, z_k), was calculated using the probability density of a normal distribution with each mean value of the previous position, x_{k-1}, y_{k-1}, and z_{k-1}, and $variance$, where $dwell = t_k - t_{k-1}$. This probability density can be expressed with mathematical format as below equations[9].

$$P(x_k|x_{k-1}) \sim Normal\left(x_{k-1}, 2(t_k - t_{k-1})\right)$$
$$P(y_k|y_{k-1}) \sim Normal\left(y_{k-1}, 2(t_k - t_{k-1})\right)$$
$$P(z_k|z_{k-1}) \sim Normal(z_{k-1}, 2(t_k - t_{k-1}))$$

Because there are three independent one dimensional random walks, each step on *x*, *y*, and *z* was generated independently. Therefore, the dimension, *n*, was 1 as input parameter during the simulation works. When the position of a molecule deviates from the range of R_{wall}, the molecule stayed at the previous position as not conducting the one displacement of the next step. Assuming the quantum yield from the excitation is 100 % for simplicity, the detection intensity of fluorescence (*I*) at location (*x, y,* and *z*) and time *t* can be expressed as below.

$$I(x,y,z,t) = I_0 \cdot exp\left(\frac{-2(x(t)^2 + y(t)^2)}{\omega_0^2}\right) \cdot exp\left(\frac{-2(z(t)^2)}{z_0^2}\right)$$

where I_0 is the fluorescence intensity at the center of the beam. The input value of I_0 was 250 for convention[22]; I_0 does not affect neither the results of diffusion. The experimental shot noise and background counts were not considered in the simulation as they don't affect the autocorrelation decay. In the computer simulation, the hopping molecules traveling through the beam area were converted to virtual photon counts dependent on their locations of Gaussian beam intensity. Each simulated five

sequent diffusion steps of 2 μs dwell time were summed to one step of 10 μs dwell time when to construct an intensity profile. A data trace of photon fluctuation was constructed to a plot of fluorescence intensity over time. The first 10,000 diffusion steps were considered as an equilibrium process from the initial generations, and they were excluded from the part of analysis. Once the photon fluctuation data was generated, the autocorrelation curve was constructed. Either the pure diffusion model or a newly designed adsorption model was used for conducting nonlinear curve fitting on the autocorrelation curve to determine the diffusion coefficient and desorption rate parameter. The purpose of the simulation was to assess how accurately and precisely we can obtain the parameter of diffusion coefficient from the mathematical fitting model on the constructed autocorrelation curve.

For clarifying the term "adsorption event", it describes a phenomenon when the diffusing molecules (adsorbate) are adsorbed to pore wall or interfacial area near the stationary phase (adsorbent), and desorption is implicitly included in this "adsorption event" because the adsorption is not permanent but temporary in general. These adsorption and desorption occur repeatedly, and this phenomenon is called as adsorption event. Therefore, the photon counting should include correct information of both pure diffusion and adsorption events. The average adsorption time (t_{ads}, the average time between two sequent adsorption events) and the average desorption time (t_{des}, the average time of holding the adsorption events) can be expressed as below equations[22].

$$\frac{1}{t_{ads}} = \lambda_{ads} = k_1 C_A = \frac{POS}{dwell}$$

$$\frac{1}{t_{des}} = \lambda_{des} = k_{-1}$$

where POS represents probability of stopping for a dwell time.

As described in Wirth's paper (2001), the fractional concentration of adsorbed molecules, f_C can be expressed with POS because the probability of stopping controls the population of adsorption events[22].

$$f_C = \frac{\frac{POS}{k_{-1} \cdot dwell}}{1 + \frac{POS}{k_{-1} \cdot dwell}}$$

Therefore, the fractional concentration of diffusing molecules, $f_B = 1 - f_C = \frac{1}{1+\frac{POS}{k_{-1} \cdot dwell}}$.

Both rates of adsorption and desorption were expected to follow Poisson statistics, therefore the distribution of these events were expected to be exponential decay as below equations[22].

$$P(t_{ads}) = exp(-t \cdot \lambda_{ads})$$

$$P(t_{des}) = exp(-t \cdot \lambda_{des})$$

Using cumulative summation of those probabilities, the random variables for adsorption and desorption steps were generated, and the populations of adsorption and desorption steps were acquired by tracking the simulation results. Constructing the histograms of those populations are important to evaluate whether the simulation has been operated as intended or not; both adsorption rate parameter ($k_1 C_A$) and desorption rate parameter (k_{-1}) as input variables should be precisely approach to the exponential decay on the histogram curve. The accuracy of predicting the output k_{-1} from the nonlinear curve fit result can be evaluated by comparing to the simulation input value of k_{-1} as following theoretical error equation.

$$Error\ (\%) = \left| \frac{k_{-1}\ simulation\ input\ -\ k_{-1}\ from\ nonlinear\ curve\ fit}{k_{-1}\ simulation\ input} \right| \times 100\ (\%)$$

4. Result and Discussion

One representative virtual intensity profile with adsorption events (simulation input: $k_{-1} = 1000\ 1/s$, $POS = 0.0005$, and $dwell = 2\ \mu s$ before constructing the intensity profile) was described in Fig. 1. The virtual intensity profile in Fig. 1A showed the photon fluctuation and an enlarged range as shown in Fig. 1B which visualized some significant adsorption events. The histogram result in Fig. 1C and Fig. 1D provided that $k_1 C_A = 256.0 \pm 0.6\ 1/s$ and $k_{-1} = 987 \pm 4\ 1/s$, and those output values were very close to the simulation input values: $k_1 C_A = \frac{0.0005}{2\ \mu s} = 250\ 1/s$ and $k_{-1} = 1000\ 1/s$. The accuracy of the histograms has been evaluated with theoretical error equation as shown in Table 1. The result from the fitting for k_{-1} and f_B were 1130 ± 20 1/s and 0.786 ± 0.005 respectively, and diffusion coefficient was held same as input simulation value (D = 6.78 × 10^{-6} cm^2/s)[20]. Fig. 2 showed a set of normalized autocorrelation curves with fitting consistent POS and varied k_{-1} (500, 1000, 2000, and 4000 1/s), and another set of consistent k_{-1} and varied POS (0.0001, 0.0005, 0.0009, and 0.0013). Overall, those curves showed a good quality of fitting which implied the prediction of the theoretical model on the realistic autocorrelation curve was satisfying. In the same way of analysis as shown in the examples in Fig. 2, there were various pairs of POS and k_{-1} to simulate and observe the

decay curve trends and the predictions on them. The summary table of k_{-1} and f_B from autocorrelation curve fits were shown in Table 1. The summary plots for theoretical error of k_{-1} and f_B were shown in Fig. 3 based on Table 1.

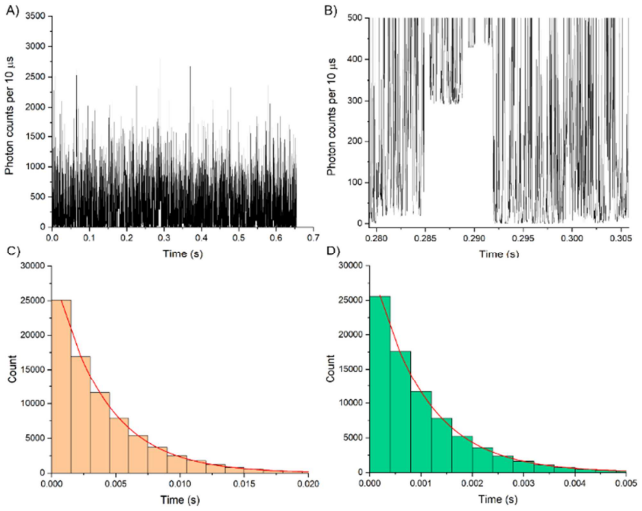

Fig. 1. The summary of simulation result with a set of input values of $k_{-1} = 1000\ 1/s$, $POS = 0.0005$. [Caption: (A) Virtual intensity profile with $dwell = 10\ \mu s$, (B) Enlarged specific part of significant adsorption events, Histogram of (C) adsorption and (D) desorption steps in time with $dwell = 2\ \mu s$. The orange and green bar graphs show the histograms of adsorption and desorption time length respectively on x-axis, and the number of counts on y-axis. The red curves on both bar graphs precisely follow to determine the adsorption and desorption rate parameters. The reason why the dwell time of the intensity profile was 5 times larger is that each 5 sequent set of the simulated dynamics, which converted to intensity, with dwell time 2 µs was merged to one intensity point with dwell time 10 µs. It is to mimic the continuous molecular dynamics while a general setup of fluorescence detection would have a certain dwell time (10 µs). The limitation to discrete the molecular dynamics was 2 µs regarding of the limited computation power.]

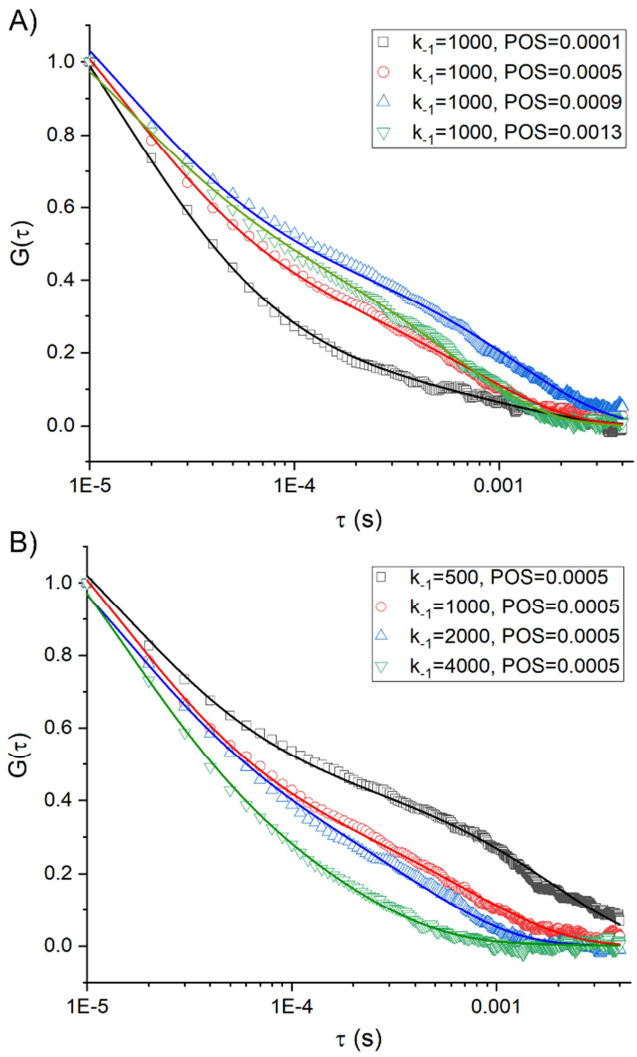

Fig. 2. Simulation result of normalized autocorrelation curves (scatter plot) and nonlinear curve fits (line plot) [Caption: (A) The combination of $k_{-1} = 1000\ 1/s$ and $POS = 0.0001$ (square, black), $k_{-1} = 1000\ 1/s$ and $POS = 0.0005$ (circle, red), $k_{-1} = 1000\ 1/s$ and $POS = 0.0009$ (upward pointing triangle, blue), and $k_{-1} = 1000\ 1/s$ and $POS = 0.0013$ (downward pointing triangle). (B) The combination of $k_{-1} = 500\ 1/s$ and $POS = 0.0005$ (square, black), $k_{-1} = 1000\ 1/s$ and $POS = 0.0005$ (circle, red), $k_{-1} = 2000\ 1/s$ and $POS = 0.0005$ (upward pointing triangle, blue), and $k_{-1} = 4000\ 1/s$ and $POS = 0.0005$ (downward pointing triangle).]

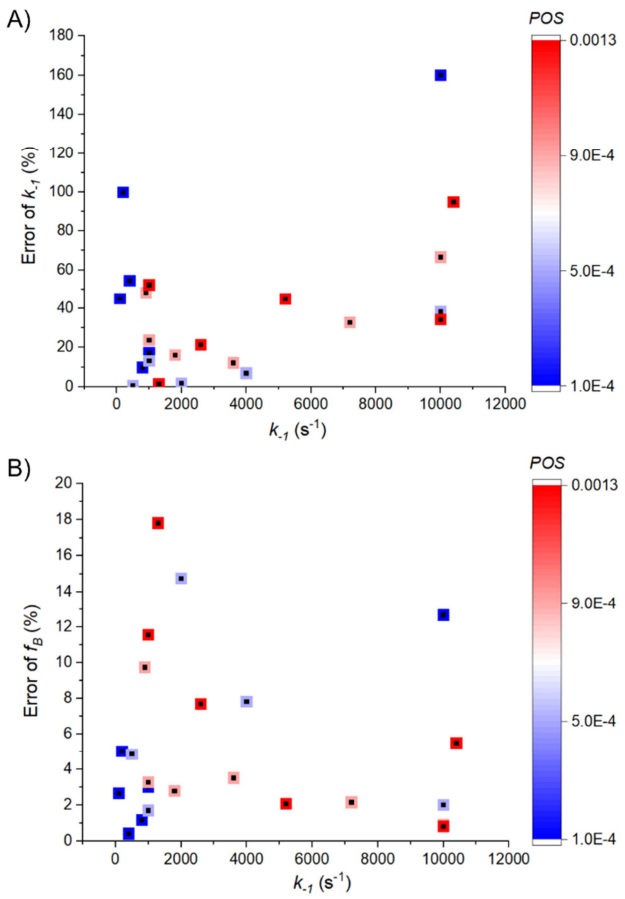

Fig. 3. Scatter plots for the relationship of k_{-1} in the simulation and theoretical errors of k_{-1}. [Caption: (A) and f_B (B), and POS in the simulation, as shown in x-axis, y-axis, and a color bar respectively. The colors are red, light red, light blue, and blue for POS of 0.0001, 0.0005, 0.0009, and 0.0013 respectively.

The Fig. 3 plot gives the idea that how much the error of k_{-1} can arise depending on both the simulation input values k_{-1} and *POS* in the photon fluctuation. The three leftmost red dots (*POS* = 0.0001) in Fig. 3A gave relatively high errors of k_{-1} than other data points, and the rightmost red dot gave the highest error of k_{-1} in the plot. The trend can be interpreted that the relatively too lower or too higher simulation values of k_{-1} (in a range of k_{-1} < 500 1/s or k_{-1} > 10000 1/s) with the relatively lower values of *POS* can give relatively high fitting errors. In contrary, the other red dots in the range of 800–1000 1/s of k_{-1} with same *POS* value gave significantly lower errors of desorption rate comparing to the former cases (range of k_{-1} < 500 1/s or k_{-1} > 10000 1/s).

The group of light red dots (*POS* = 0.0005) gave the significantly lower errors of k_{-1} comparing to the other data points except the rightmost light red dot which appeared relatively high (40 %) error. The group of light blue dots (*POS* = 0.0009) gave relatively higher errors of k_{-1} than the group of light red dots, and there was no specific trend of errors for the group of blue dots (*POS* = 0.0013). The common trend of each set of color dots showed the higher errors when the k_{-1} is either extremely low (100–500 s^{-1}) or extremely high (>7000 s^{-1}).

When those two extreme cases come with fluctuation plot from the simulation, they can be understood intuitively. In the extremely low k_{-1} with extremely low *POS* condition, the width of desorption time will cover too long range in the data trace and only few cases of adsorption events will appear; the capacity of one data trace only includes the time length of 655.35 ms. For example, 100 1/s of k_{-1} represents that the one molecule will be adsorbed at one random location for 10 ms long in average that appears in a data trace, which might be too long to distinguish other overlapped individual adsorption events. Another problem comes when there are only few cases of adsorption events longer than 50 ms because of the low *POS*, and probably the capacity of one trace is not enough to include all the information to illustrate k_{-1} and *POS*. The relatively high errors (12–19 %) in histogram fits for the low POS (0.0001) group in Table 1 verified that there were relatively insufficient adsorption events in a data trace. Therefore, the analysis of autocorrelation may not be accurately interpreted when having low *POS*. The combinations of k_{-1} and *POS* in shaded cells with gray color (Table 1) were excluded from the plot of Figure 3, because they are not satisfying the assumption of adsorption model; $k_1 C_A$ should be significantly smaller than k_{-1}.

The statistical comparison of two models (pure diffusion "model 1" and adsorption "model 2") was conducted by *F*-test with three examples in Fig. 4 (*example-1* and *example-2,* and *example-3*). Those three examples come from the simulation with input pairs of k_{-1} = 1000 1/s and *POS* = 0.0001 (*example-1*, Fig. 4A and 4B), k_{-1} = 1000 1/s and *POS* = 0.0013 (*example-2,* Fig. 4C and 4D), and k_{-1} = 10000 1/s and *POS* = 0.0001 (*example-3*, Fig. 4E and 4F). The *F*-test of each example and model was done for the first 50 data points ($n = 50$) because the fitting quality from the early part is where to mostly affect the nonlinear curve fits. D = 6.78 × 10^{-6} cm^2/s was constant input parameter for both models when they were fitted. The two models have different number of fitting parameters: N for pure diffusion model (model 1, $number\ of\ fitting\ parameters = 1$) and N, k_{-1}, and f_B for adsorption model (model 2, $number\ of\ fitting\ parameters = 3$). Therefore, *F*-test

equation on model 1 (pure diffusion model) and model 2 (adsorption model) is following equation.

$$F = \frac{\frac{(RSS_1 - RSS_2)}{(p_2 - p_1)}}{\frac{RSS_2}{(n - p_2)}}$$

where RSS represents residual sum of squares. The residual data was transferred from the fitting result of OriginPro. The critical value of $F(v_1, v_2, \alpha) = F(2, 46, 0.05) = 3.195$, where numerator degrees of freedom and denominator degrees of freedom are $v_1 = p_2 - p_1$ and $v_2 = n - p_2$ respectively, and $\alpha = 0.05$ for 5 % significant level of one-sided tail test; we expect the more complex model, so model 2 should be better fitting model than model 1. The summary of *F*-test for the three examples was described in Table 2. The RSS values in two models from *example-1* showed a big difference in values, 0.3559 at model 1 and 0.003985 at model 2. Clearly this led to the calculated *F* value, 2075, which is much higher than the critical *F* value, 3.195. This meant the adsorption model showed significantly better nonlinear curve fitting on the autocorrelation curve. The RSS values in two models from *example-2* showed a large difference in values, 4.488 at model 1 and 0.008929 at model 2. Clearly this led to the calculated *F* value, 11790, which is much higher than the critical *F* value, 3.195. This meant the adsorption model showed significantly better nonlinear curve fitting on the autocorrelation curve. The RSS values in *example-3* showed relatively smaller gap between model 1 and model 2 which led to the small, calculated *F* value, 1.400. Because the critical *F* value was not higher than the calculated *F* value in this case, it indicated that the fitting quality of model 1 showed competitively good quality as model 2 showed. The adsorption model was not necessary in this case and the parameters in the adsorption model were not expected to provide useful information.

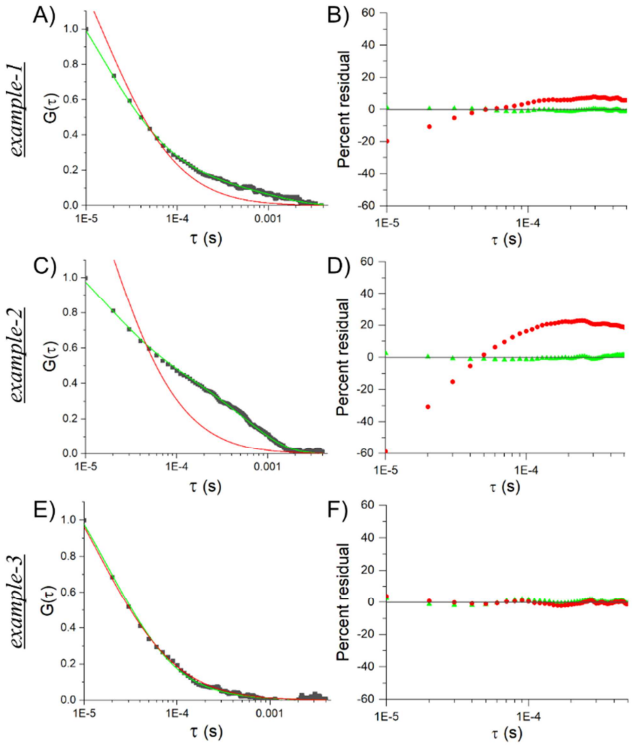

Fig. 4 Three representative examples for comparison of fitting quality between model 1 (pure diffusion model, red) and model 2 (adsorption model, green). [Caption: Those three examples are called *example-1* (k_{-1} = 1000 1/s, *POS* = 0.0001) and *example-2* (k_{-1} = 1000 1/s, *POS* = 0.0013), and *example-3* (k_{-1} = 10000 1/s, *POS* = 0.0001). The left-side column of the figure (A, C, and E) are three plots of nonlinear curve fitting on autocorrelation data with model 1 (red) and model 2 (green). The right-side column of the figure (B, D, and F) are three plots of percent residual from the fitting results.]

Table 1. Summary of simulation for diffusion and adsorption events in the 3-D virtual confocal system results

[Caption: The boundary of two groups was indicated by a thick line between two rows in the chart. There were two duplicated combinations (marked as *) of POS and k_{-1} (s^{-1}) because of showing two different comparison groups in convention. Those filled with gray color in the table deviated the assumptions of strong rare adsorption, so those sets were not included in Fig. 3.]

Simulation input values		Output of autocorrelation curve fit		Theoretical error of histogram curve fit	
POS	k_{-1}	k_{-1}	f_B	k_{-1} %	$k_1 C_A$ %
*0.0001	100	$(5.48_4 \pm 0.09_7)$ E+01	$0.684_5 \pm 0.002_5$	18.80	2.62
0.0001	200	$(3.99_4 \pm 0.04_7)$ E+02	$0.759_8 \pm 0.004_1$	16.40	3.20
0.0001	400	$(6.18 \pm 0.1_3)$ E+02	$0.892_7 \pm 0.002_5$	14.00	1.28
0.0001	800	$(7.2_1 \pm 0.2_6)$ E+02	$0.952_3 \pm 0.001_6$	13.54	0.29
0.0005	500	$(5.03_7 \pm 0.04_3)$ E+02	$0.699_1 \pm 0.004_7$	2.52	0.10
*0.0005	1000	$(1.13_3 \pm 0.01_7)$ E+03	$0.786_3 \pm 0.004_8$	2.41	1.28
0.0005	2000	$(2.03_6 \pm 0.03_1)$ E+03	$0.757_9 \pm 0.005_9$	2.08	0.37
0.0005	4000	$(4.2_8 \pm 0.1_6)$ E+03	$0.867_7 \pm 0.007_6$	2.97	2.35
0.0009	900	$(4.64_8 \pm 0.05_4)$ E+02	$0.731_6 \pm 0.005_2$	1.38	0.60
0.0009	1800	$(1.51_0 \pm 0.02_0)$ E+03	$0.822_3 \pm 0.003_4$	0.64	0.74
0.0009	3600	$(3.1_6 \pm 0.1_1)$ E+03	$0.857_6 \pm 0.007_4$	0.96	1.10
0.0009	7200	$(4.8_4 \pm 0.6_1)$ E+03	$0.961_6 \pm 0.006_9$	1.16	3.33
0.0013	1300	$(1.279_1 \pm 0.009_5)$ E+03	$0.547_9 \pm 0.007_7$	0.06	0.46
0.0013	2600	$(2.04_6 \pm 0.04_6)$ E+03	$0.861_6 \pm 0.004_2$	0.44	1.09
0.0013	5200	$(2.86_3 \pm 0.07_7)$ E+03	$0.870_3 \pm 0.004_9$	0.87	2.37
0.0013	10400	$(5.3_0 \pm 1.0_0)$ E+02	$0.993_0 \pm 0.001_0$	0.74	4.00
*0.0001	100	$(5.48_4 \pm 0.09_7)$ E+01	$0.684_5 \pm 0.002_5$	18.80	2.62
0.0005	100	$(6.21_4 \pm 0.04_7)$ E+01	$0.397_4 \pm 0.003_9$	7.64	0.92
0.0009	100	$(1.082_3 \pm 0.001_1)$ E+02	$0.162_1 \pm 0.001_6$	4.07	1.70
0.0013	100	$(3.998_5 \pm 0.005_1)$ E+01	$0.060_2 \pm 0.001_1$	5.86	0.97
0.0001	1000	$(8.2_8 \pm 0.2_1)$ E+02	$0.923_7 \pm 0.002_1$	15.60	0.84
*0.0005	1000	$(1.13_3 \pm 0.01_7)$ E+03	$0.786_3 \pm 0.004_8$	2.41	1.28
0.0009	1000	$(7.62_1 \pm 0.06_9)$ E+02	$0.712_2 \pm 0.004_8$	1.44	0.37
0.0013	1000	$(1.52_3 \pm 0.01_3)$ E+03	$0.676_1 \pm 0.005_2$	1.34	0.20
0.0001	10000	$(2.5_6 \pm 0.3_1)$ E+04	$0.86_9 \pm 0.02_4$	12.00	4.36
0.0005	10000	$(6.1_5 \pm 0.7_7)$ E+03	$0.955_9 \pm 0.008_9$	1.22	3.15
0.0009	10000	$(3.3_4 \pm 0.2_2)$ E+03	$0.948_1 \pm 0.004_4$	1.14	4.04
0.0013	10000	$(6.5_7 \pm 0.6_8)$ E+03	$0.946_7 \pm 0.009_3$	0.65	3.93

Table 2. *F*-statstics comparison for two models: pure model (model 1) versus adsorption model (model 2).

	RSS	Calculated *F* value
example-1 with model 1	0.3559	2075
example-1 with model 2	0.003985	
example-2 with model 1	4.488	11790
example-2 with model 2	0.008929	
example-3 with model 1	0.007917	1.400
example-3 with model 2	0.007472	

5. Conclusion

The mathematical model for interpreting the autocorrelated fluctuation data was tested by generating Monte Carlo simulation. The computer simulation combined Brownian motion and random stopping-departing motion. Based on the simulation result, the range of desorption rate (800–1000 1/s) was where the analytical model confidently predicts both diffusion and adsorption-desorption dynamics. The limitation of predicting adsorption and desorption rates was discussed; either too small amount of adsorption events or too short adsorption and desorption time in the data trace will limit the accuracy prediction. The theoretical autocorrelation model is expected to reveal not only the diffusion but also the adsorption-desorption kinetics in the porous environment, which are essential towards developing a better understanding of the origin of the resolution limit in chemical separation science.

Acknowledgement

I acknowledge my academic advisor, Professor Max Lei Geng at University of Iowa, Chemistry department. He introduced me to this field of study and the paper of Wirth et al. (2001), so that I could start to read all the related sources and I could decide to initiate and develop this contribution. The advice to add statistical analysis was appreciated.

Reference

1. Magde, D., E. Elson, and W.W. Webb, *Thermodynamic Fluctuations in a Reacting System---Measurement by Fluorescence Correlation Spectroscopy.* Physical Review Letters, 1972. **29**(11): p. 705-708.
2. Magde, D., E.L. Elson, and W.W. Webb, *Fluorescence correlation spectroscopy. II. An experimental realization.* Biopolymers, 1974. **13**(1): p. 29-61.
3. Elson, E.L. and D. Magde, *Fluorescence correlation spectroscopy. I. Conceptual basis and theory.* Biopolymers, 1974. **13**(1): p. 1-27.
4. Hansen, R.L. and J.M. Harris, *Measuring Reversible Adsorption Kinetics of Small Molecules at Solid/Liquid Interfaces by Total Internal Reflection Fluorescence Correlation Spectroscopy.* Analytical Chemistry, 1998. **70**(20): p. 4247-4256.
5. Elson, E.L., *Fluorescence correlation spectroscopy: past, present, future.* Biophys J, 2011. **101**(12): p. 2855-70.
6. Haustein, E. and P. Schwille, *Fluorescence correlation spectroscopy: novel variations of an established technique.* Annu Rev Biophys Biomol Struct, 2007. **36**: p. 151-69.
7. Yu, L., et al., *A Comprehensive Review of Fluorescence Correlation Spectroscopy.* Frontiers in Physics, 2021. **9**.
8. Banks, D.S., et al., *Characterizing anomalous diffusion in crowded polymer solutions and gels over five decades in time with variable-lengthscale fluorescence correlation spectroscopy.* Soft Matter, 2016. **12**(18): p. 4190-203.
9. Jazani, S., et al., *An alternative framework for fluorescence correlation spectroscopy.* Nat Commun, 2019. **10**(1): p. 3662.
10. Neuweiler, H., et al., *Dynamics of unfolded polypeptide chains in crowded environment studied by fluorescence correlation spectroscopy.* J Mol Biol, 2007. **365**(3): p. 856-69.
11. Lee, H.B., et al., *Rotational and translational diffusion of size-dependent fluorescent probes in homogeneous and heterogeneous environments.* Phys Chem Chem Phys, 2018. **20**(37): p. 24045-24057.
12. National Academies of Sciences, E. and

Medicine, *A Research Agenda for Transforming Separation Science*. 2019, Washington, DC: The National Academies Press. 114.
13. Wirth, M.J. and M.A. Legg, *Single-molecule probing of adsorption and diffusion on silica surfaces.* Annu Rev Phys Chem, 2007. **58**: p. 489-510.
14. Wirth, M.J., M.D. Ludes, and D.J. Swinton, *Spectroscopic Observation of Adsorption to Active Silanols.* Analytical Chemistry, 1999. **71**(18): p. 3911-3917.
15. Gritti, F. and G. Guiochon, *Mass transfer kinetics, band broadening and column efficiency.* J Chromatogr A, 2012. **1221**: p. 2-40.
16. Gritti, F. and G. Guiochon, *Influence of the degree of coverage of C18-bonded stationary phases on the mass transfer mechanism and its kinetics.* J Chromatogr A, 2006. **1128**(1-2): p. 45-60.
17. Ries, J. and P. Schwille, *Fluorescence correlation spectroscopy.* Bioessays, 2012. **34**(5): p. 361-8.
18. Ries, J., E.P. Petrov, and P. Schwille, *Total internal reflection fluorescence correlation spectroscopy: effects of lateral diffusion and surface-generated fluorescence.* Biophys J, 2008. **95**(1): p. 390-9.
19. Petrasek, Z. and P. Schwille, *Precise measurement of diffusion coefficients using scanning fluorescence correlation spectroscopy.* Biophys J, 2008. **94**(4): p. 1437-48.
20. Zhong, Z., et al., *Probing strong adsorption of solute onto C18-silica gel by fluorescence correlation imaging and single-molecule spectroscopy under RPLC conditions.* Anal Chem, 2005. **77**(8): p. 2303-10.
21. Lee, H., ; Geng, M. L., *Imaging diffusion and adsorption in chromatographic nanoporous silica particles with fluorescence correlation spectroscopy.* Submitted to ACS Measurement Science Au, 2023.
22. Wirth, M.J., M.D. Ludes, and D.J. Swinton, *Analytic Solution to the Autocorrelation Function for Lateral Diffusion and Rare Strong Adsorption.* Applied Spectroscopy, 2001. **55**(6): p. 663-669.
23. Aragón, S.R. and R. Pecora, *Fluorescence correlation spectroscopy as a probe of molecular dynamics.* The Journal of Chemical Physics, 1976. **64**(4): p. 1791-1803.
24. Eigen, M. and R. Rigler, *Sorting single molecules: application to diagnostics and evolutionary biotechnology.* Proc Natl Acad Sci U S A, 1994. **91**(13): p. 5740-7.
25. Ries, J., et al., *A comprehensive framework for fluorescence cross-correlation spectroscopy.* New Journal of Physics, 2010. **12**(11): p. 113009.